Changes to the Atmospheric Correction Algorithm and Retrieval of Oceanic Optical Properties

Bryan A. Franz
Science Applications International Corporation
Beltsville, Maryland

Sean W. Bailey
Futuretech Corporation
Greenbelt, Maryland

Robert E. Eplee, Jr.
Science Applications International Corporation
Beltsville, Maryland

Menghua Wang
University of Maryland, Baltimore County
Baltimore, Maryland

Abstract

This chapter describes a number of algorithm changes which were implemented in the fourth SeaWiFS reprocessing to enhance the performance of the atmospheric correction process and improve the quality and consistency of oceanic optical property retrievals.

5.1 Introduction

While the general approach to SeaWiFS atmospheric correction over oceans has not changed for the fourth SeaWiFS reprocessing, a number of refinements were implemented and evaluated. Several of these modifications were found to yield significant improvement in the quality and consistency of oceanic optical property retrievals, and were included in the final reprocessing software. The changes include a filtering scheme for the reduction of aerosol model selection noise, a modification to improve algorithm performance in very clear atmospheres, updates to the corrections for out-of-band response, an extension of the water-leaving radiance normalization to account for Fresnel transmittance through the air-sea interface, and a fix for aerosol model ambiguity problems. These changes are detailed in the sections that follow.

5.2 NIR Relative Noise Reduction

The SeaWiFS atmospheric correction algorithm (Gordon and Wang 1994) relies on the single-scattering aerosol reflectance ratio (epsilon, ε) between the two near-infrared (NIR) bands at 765 and 865 nm to select the aerosol type. The atmospheric correction is, therefore, highly sensitive to any relative noise between these two NIR channels. A filtering technique was developed to reduce the relative noise in the NIR band ratio, which thereby reduces the small-scale variability in aerosol model selection. The

smoothing filter adjusts the radiance in the 765 nm channel to minimize local variability in the observed NIR aerosol ratio (i.e., the multiscattering equivalent of atmospheric epsilon, ε_{ms}), while leaving the 865 nm radiance (which governs aerosol concentration) unchanged. The effect of this smoothing is to reduce pixel-to-pixel variability in the retrieved aerosol type, which ultimately reduces atmospheric correction noise in the retrieved water-leaving radiances.

The effect of this filtering can easily be seen in Level-2 images of epsilon, Angstrom coefficient, and, to a lesser extent, aerosol optical thickness at 865 nm. The value of this smoothing will diminish with increasing spatial and temporal averaging, and is more readily seen as reduced speckling in Level-2 oceanic and atmospheric optical property retrievals. The smoothing has been found to induce no bias-change in either the aerosol optical thickness or the water-leaving radiances.

The smoothing algorithm is as follows:

1) Define NIR aerosol radiance at pixel i for wavelength λ as

$$L_a(\lambda,i) = [\ (L_t(\lambda,i) - tL_f(\lambda,i))/t_{oz}(\lambda,i) - L_r(\lambda,i)\ ]/t_{ox}(\lambda,i);$$

2) Given a scan/pixel window centered on pixel x, containing a total of n unmasked pixels, compute mean $L_a(\lambda)$ at x as

$$<L_a(\lambda,x)> = 1/n\ \ \Sigma\ L_a(\lambda,i),\ \ \text{for i=1,n and } \lambda\text{=765 or 865nm;}$$

3) Compute mean, multiscattering epsilon at pixel x as

$$\varepsilon_{ms} = <L_a(765,x)> / <L_a(865,x)>;$$

4) Now compute a new $L_a(765,x)$ which would yield the mean epsilon when combined with the original $L_a(865,x)$

$$L_a'(765,x) = \varepsilon_{ms}\ L_a(865,x);$$

5) Reconstruct the top of atmosphere (TOA) radiance at 765nm as

$$L_t(765,x) = [L_a'(765,x)\ t_{ox}(765,x) + L_r(765,x)]\ t_{oz}(765,x) + tL_f(765,x);$$

where:

$L_t(\lambda,i)$ is the observed TOA radiance for wavelength λ at pixel i,
$tL_f(\lambda,i)$ is the white-cap radiance, transmitted to the TOA,
$L_r(\lambda,i)$ is the Rayleigh path radiance,
$L_a(\lambda,i)$ is the aerosol path radiance, including Rayleigh-aerosol interaction,
$t_{ox}(\lambda,i)$ is the oxygen transmittance,
$t_{oz}(\lambda,i)$ is the ozone transmittance.

Using the filter-adjusted TOA radiance at 765 nm, the SeaWiFS atmospheric correction algorithm is then operated in the standard manner.

It is desirable to keep the filter window size as small as possible, to limit the reduction of real changes in aerosol type. The window size, however, needs to be large enough to

allow sufficient sample size for the averaging to be effective. In addition to varying the size, it is also possible to change the shape. This can be achieved by introducing the concept of a filter window kernel, which indicates which pixels within the window will be considered in computing the filtered value. Consider these two examples of a 5x5 filtering window, where the value of 1 indicates that the pixel at that location will contribute.

Square 5x5					Diamond 5x5				
1	1	1	1	1	0	0	1	0	0
1	1	1	1	1	0	1	1	1	0
1	1	1	1	1	1	1	1	1	1
1	1	1	1	1	0	1	1	1	0
1	1	1	1	1	0	0	1	0	0

For the same window size, the diamond filter kernel reduces the number of contributing samples by approximately 50% over the square kernel, and the radius of influence is never greater than two pixels. While this reduces the number of samples contributing to the mean, the diamond shape is better designed to minimize line-by-line digitization problems such as those associated with SeaWiFS mirror-side differences. This is because the diamond kernel gives nearly equal weight to the odd and even lines, while the square kernel yields a 3-to-2 over-weighting of opposing lines.

For SeaWiFS local area coverage (LAC) resolution data, it was found that the NIR relative noise reduction filter with a 5x5 diamond kernel gave the best compromise between noise reduction and aerosol smoothing. Figure 1 shows a LAC subscene of L_{WN} at 443 nm, before and after smoothing.

Unfortunately, it was found that the filtering approach did not always reduce noise in SeaWiFS global area coverage (GAC) resolution scenes. The problem appears to be that the GAC data set, being subsampled at the sensor, does not contain a complete record of the bright sources observed by the instrument. This is a fundamental limitation of SeaWiFS, as it is simply not possible to identify and correct for all stray light contamination in the GAC data set. Any algorithm which combines neighboring pixels will, therefore, increase the probability of stray light contamination in a given pixel. The problem is most significant in the vicinity of scattered clouds. Considering this limitation, and the fact that GAC data are primarily used for generating spatial and temporal composites (where noise will be significantly reduced through averaging), it was decided that the NIR relative noise reduction filter would not be applied to the GAC products in this reprocessing.

5.3 Clear Atmospheric Conditions

Under very clear atmospheric conditions, the Rayleigh-subtracted radiance in the NIR approaches zero. When other uncertainties are included, the retrieved aerosol path radiances in the NIR may even go slightly negative. The aerosol model selection, therefore, becomes highly uncertain in clear atmospheric conditions. As a result, the

SeaWiFS atmospheric correction algorithm often fails to obtain ocean-color retrievals in the best of atmospheric conditions. A simple solution to this problem is to fix the aerosol type when the aerosol path radiance in one or both of the NIR bands approaches zero, and limit the aerosol radiance at 865 nm to be greater than or equal to zero. With these two changes, it is possible for the atmospheric correction algorithm to procede when the retrieved aerosol concentration is effectively zero.

The aerosol type to which low aerosol pixels will be fixed is a simple white aerosol, i.e., $\rho_a(\lambda) = \rho_a(865)$, where $\rho_a(\lambda)$ is aerosol path reflectance at wavelength λ. The threshold below which the aerosol model will be fixed has been set at a very conservative value of ρ_a (NIR) = 0.0001. For the 765 and 865 nm channels, this reflectance value corresponds to slightly greater than 1 digital count. Raising this value will force a larger percentage of the pixels to assume white aerosols, thus bypassing the aerosol model selection process of Gordon and Wang (1994).

In conjunction with the above enhancement, the occurrence of $[(L_t\text{-}tL_f)/t_{oz} - L_r) < 0]$ in one or more of bands 2-8 will no longer be considered an atmospheric correction failure condition.

5.4 Out-of-band Correction

The SeaWiFS spectral bands cover the range from 380 to 1150 nm, with nominal band centers at 412, 443, 490, 510, 555, 670, 765, and 865 nm. The spectral bandwidth, which is defined as the full width at half the maximum response, is 20 nm for the first six bands and 40 nm for the two NIR bands. The SeaWiFS bands, however, are known to exhibit significant response well beyond the quoted spectral range of the bandpasses. Throughout the SeaWiFS atmospheric correction process, adjustments are made to account for this out-of-band response (Gordon 1995). In the third SeaWiFS reprocessing, additional corrections were added to adjust the retrieved L_{WN} values to correspond to the nominal band center wavelengths (Wang et al. 2001). For the fourth SeaWiFS reprocessing, several modifications were made to the out-of-band corrections for the water-leaving radiances and derived reflectances. These changes are discussed in the sections that follow.

5.4.1 Remote-Sensing Reflectance

The solar irradiance (F0) values used in the SeaWiFS atmospheric correction processing are band-averaged quantities. This means that the solar spectrum has been convolved with the relative spectral response (RSR) function, where the RSR may include significant out-of-band response. In the third SeaWiFS reprocessing, an algorithm was introduced to correct the L_{WN} retrievals from band-averaged quantities to a nominal wavelength. Unfortunately, the out-of-band corrected L_{WN} was still normalized by the band-averaged F0 when computing remote-sensing reflectance, Rrs. Rrs ratios between the visible bands were then used as input to the OC4 chlorophyll algorithm (O'Reilly et al. 2000), so the resulting chlorophyll retrievals may have been slightly biased. In the

fourth reprocessing, the nominal-band L_{WN} values were normalized by nominal-band F0 values when computing Rrs.

5.4.2 Water-Leaving Radiance

The L_{WN} retrievals are computed as band-averaged values, with an out-of-band correction applied prior to use in downstream computations such as chlorophyll retrieval. The correction applied in the third SeaWiFS reprocessing was computed from the Band 3-to-Band 5 ratio, and was based on a chlorophyll-dominated L_{WN} spectrum which uses the Gordon et al. (1988) model. A revised set of correction factors were generated for this reprocessing using the recently published clear-water reflectance model of Morel and Maritorena (2001). Figure 2 shows the comparison between the correction factors from Gordon et al. (1988) and Morel and Maritorena (2001), with the Morel and Maritorena (2001) model results indicated by the solid lines.

This change to the out-of-band correction factors results in a lowering of chlorophyll values in waters with a Band 3-to-Band 5 L_{WN} ratio of greater than about 2. For lower ratios, chlorophyll increases slightly. Differencing tests on global binned products indicate that the revised out-of-band correction results in a net decrease of 2.5% to 4% in global averaged chlorophyll retrievals.

5.5 Fresnel Transmittance Correction

The normalization of water-leaving radiance was modified to include a correction for Fresnel transmittance through the water-atmosphere interface. The Gordon and Wang (1994) atmospheric correction algorithm assumes that the water-leaving radiance just beneath the ocean surface, L_{WN}^{-}, is uniform. For a flat ocean surface, the normalized water-leaving radiance just above the surface, L_{WN}, can be related to the value just beneath the surface as

$$nL_w(\theta) = \frac{T_f(\theta)}{n_w^2} nL_{w}^{-},$$

where θ, $T_f(\theta)$, n_w are the sensor zenith angle, the Fresnel transmittance of the air-sea interface, and the refractive index of the water, respectively. It is assumed in the above that the normalized water-leaving radiance just beneath the surface, L_{WN}^{-}, is uniform (independent of the sensor zenith angle θ). Without correction, therefore, the SeaWiFS-derived normalized water-leaving radiance, L_{WN}, depends on the sensor zenith angle according to $T_f(\theta)$. In fact, the Fresnel transmittance effect is part of the ocean bidirectional reflectance factors (f/Q correction) discussed by Morel and Mueller (2002). A simple correction was implemented to remove the air-sea transmittance effect on the SeaWiFS-derived normalized water-leaving radiances. The corrected values, $L_{WN}^{(c)}$, are computed as

$$L_{WN}^{(c)} = \frac{T_f(\theta = 0)}{T_f(\theta)} L_{WN}(\theta),$$

where $L_{WN}^{(c)}$ and L_{WN} are normalized water-leaving radiances with and without surface transmittance correction, respectively. The $L_{WN}^{(c)}$ values (for all 6 visible bands) are now the SeaWiFS-derived normalized water-leaving radiances. Note that the correction does not affect the SeaWiFS chlorophyll-a concentration values because the transmittance effects are cancelled with the two-band ratio in the normalized water-leaving radiances.

The general effect of this change is to increase the normalized water-leaving radiance in all bands, with the largest increase occurring at the highest view zenith angle, reaching approximately 3% at the GAC limit of 56-deg. Figure 3 shows the effect of this Fresnel correction across the full SeaWiFS scan. The scan trends were derived by simple averaging of water-leaving radiance retrievals within each scan pixel over a 1-year period in the relatively homogeneous waters near Hawaii. The solid line is the corrected data, the dashed is uncorrected. Note that the roll-off in radiance near the edge of the GAC swath and beyond is reduced.

5.6 Aerosol Model Ambiguity Correction

Under certain geometric conditions, the T99 (tropospheric, 99% relative humidity) and C50 (coastal, 50% relative humidity) aerosol models cross-over in epsilon space, causing discontinuities when the aerosol path radiances are extrapolated into the visible. These discontinuities appear along lines of constant scattering angle, and they are sometimes visible in images of water-leaving radiance and even chlorophyll. Application of the aforementioned NIR relative noise reduction filtering makes these effects even more apparent, as the aerosol model-selection noise is reduced across the scattering-angle isolines. A fix has been developed which identifies these model cross-over conditions and revises the model selection result accordingly. The details of these effects are discussed in Wang (2002). This is a relatively rare problem which will not significantly effect global results.

References

Gordon, H.R., O.B. Brown, R.H. Evans, J.W. Brown, R.C. Smith, K.S. Baker, and D.K. Clark, 1988: A semianalytic radiance model of ocean color. *J. Geophys. Res.*, 93, 10,909-10,924.

Gordon, H.R., and Wang, M., 1994: Retrieval of water-leaving radiance and aerosol optical thickness over the oceans with SeaWiFS: a preliminary algorithm. *Appl. Opt*. 33:443-452.

Gordon, H.R., 1995: Remote sensing of ocean color: a methodology for dealing with broad spectral bands and significant out-of-band response. *Appl. Opt*, 34, 8363-8374.

Morel, A., and S. Maritorena, 2001: Bio-optical properties of oceanic waters: A reappraisal. *J. Geophys. Res.*, 106, 7163-7180.

Morel, A., and J.L. Mueller, 2002: “Normalized water-leaving radiance and remote sensing reflectance: Bidirectional reflectance and other factors.” in: J.L. Mueller and G.S. Fargion, Eds., Ocean Optics Protocols for Satellite Ocean Color Sensor Validation, Revision 3, Vol. 2. NASA Tech. Memo. 2002-210004, NASA Goddard Space Flight Center, Greenbelt, MD, 183-210.

O'Reilly, J.E., S. Maritorena, D.A. Siegel, M.C. O'Brien, D. Toole, B.G. Mitchell, M. Kahru, F.P. Chavez, P. Strutton, G.F. Cota, S.B. Hooker, C.R. McClain, K.L. Carder, F. Muller-Karger, L. Harding, A. Magnuson, D. Phinney, G.F. Moore, J. Aiken, K.R. Arrigo, R. Letelier, and M. Culver, 2000: "Ocean color chlorophyll a algorithms for SeaWiFS, OC2, and OC4: Version 4." in: J.E. O'Reilly and co-authors, SeaWiFS Postlaunch Calibration and Validation Analyses, Part 3. NASA Tech. Memo. 2000-206892, Vol. 11, S.B. Hooker and E.R. Firestone, Eds., NASA Goddard Space Flight Center, Greenbelt, Maryland, 9-23.

Wang, M., B.A. Franz, R.A. Barnes, and C.R. McClain, 2001: Effect of spectral bandpass on SeaWiFS-retrieved near-surface optical properties of the ocean. *Appl. Opt.*, Vol. 40, No. 3, 343-348.

Wang, M., 2002: Correction of artifacts in the SeaWiFS atmospheric correction: Removing the discontinuity in the derived products, *Remote Sens. Environ.* (Submitted).

Figure Captions

Figure 1. Sample LAC image of normalized water-leaving radiance at 443 nm, before and after application of the NIR relative noise reduction filter. Panel 1a shows the scene without filtering, and panel 1b shows the same scene with filtering applied.

Figure 2. Comparison of Morel and Maritorena (2001) bio-optical model with Gordon et al. 1988 model.

Figure 3. Mean along-scan normalized water-leaving radiances retrievals, before and after application of the Fresnel transmittance correction. Solid line is with correction.

Symbols Used

$L_t(\lambda,i)$	Observed TOA radiance for wavelength λ at location i
$tL_f(\lambda,i)$	White-cap radiance, transmitted to the TOA
$L_r(\lambda,i)$	Rayleigh path radiance
$L_a(\lambda,i)$	Aerosol path radiance, including Rayleigh-aerosol interaction
$t_{ox}(\lambda,i)$	Oxygen transmittance
$t_{oz}(\lambda,i)$	Ozone transmittance
$\rho_a(\lambda)$	Aerosol path reflectance at for wavelength λ
ε	Atmospheric epsilon, ratio of single-scattering aerosol reflectances in NIR
ε_{ms}	Multiscattering equivalent of ε
F0	Solar irradiance
Rrs	Remote sensing reflectance
L_{WN}	Normalized water-leaving radiance
L_{WN}^{-}	Normalized water-leaving radiance, just below the sea surface
θ	Sensor zenith angle
$T_f(\theta)$	Fresnel transmittance of the air-sea interface
n_w	Refractive index of the water

Glossary

NIR	Near Infrared
TOA	Top-Of-Atmosphere
LAC	Local Area Coverage (SeaWiFS 1-km resolution)
GAC	Global Area Coverage (SeaWiFS 1-km resolution, subsampled to 4-km)
RSR	Relative Spectral Response

Figure Captions

Figure 1. Sample LAC image of normalized water-leaving radiance at 443 nm, before and after application of the NIR relative noise reduction filter. Panel a shows the scene without filtering, and panel b shows the same scene with filtering applied.

Figure 2. Comparison of the Morel and Maritorena (2001) bio-optical model with the Gordon et al. (1988) model.

Figure 3. Mean along-scan normalized water-leaving radiances retrievals, before and after application of the Fresnel transmittance correction. The solid is with correction.

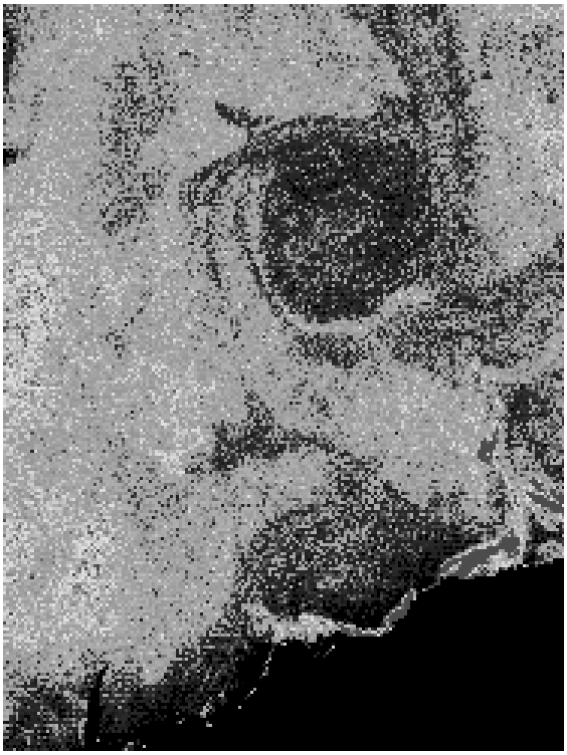

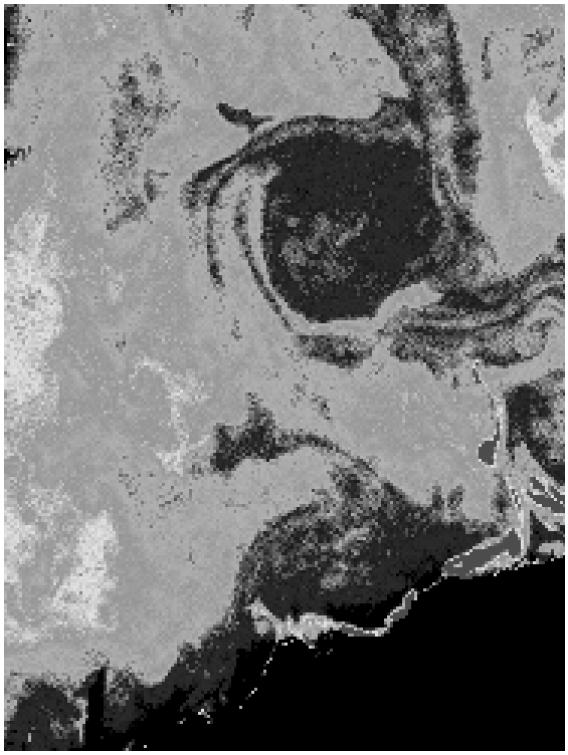

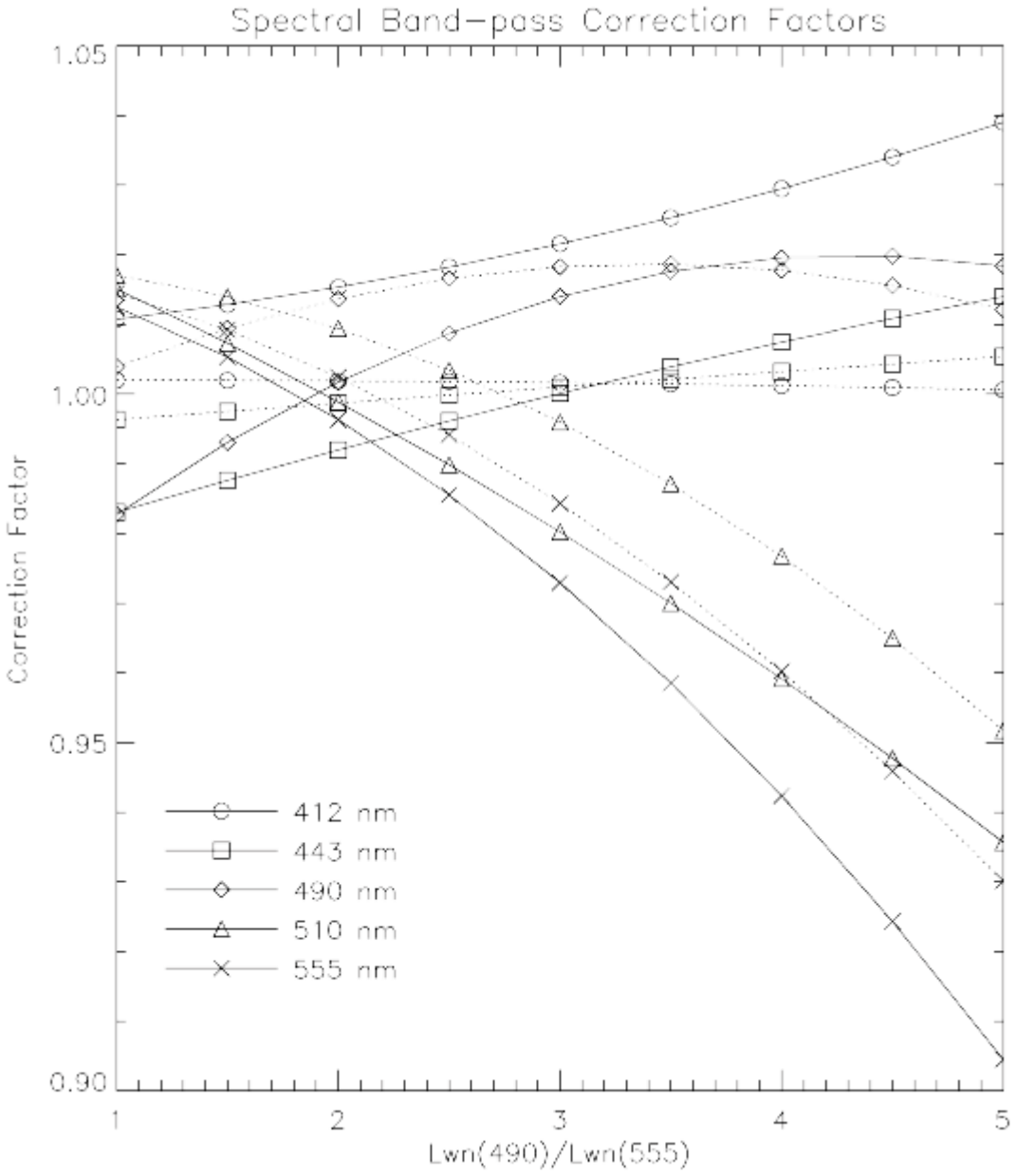
Spectral Band-pass Correction Factors
1.05
1.00
0.95
0.90
Correction Factor
412 nm
443 nm
490 nm
510 nm
555 nm
1
2
3
4
5
Lwn(490)/Lwn(555)

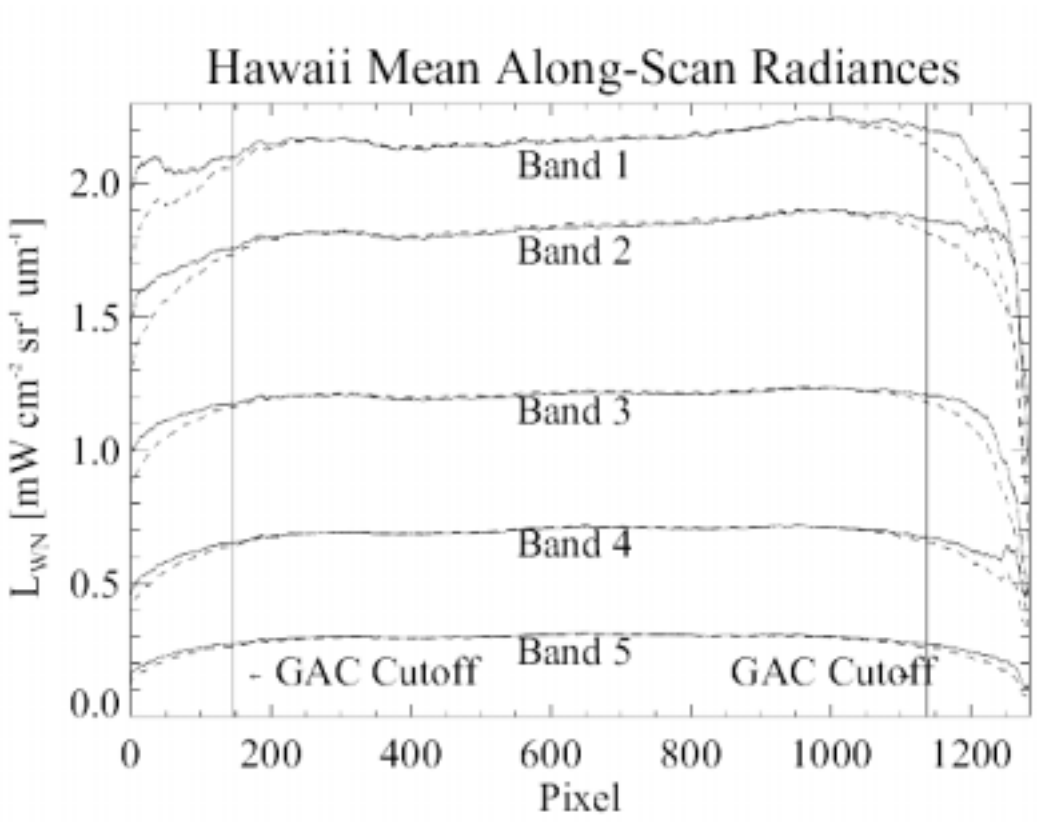
Hawaii Mean Along-Scan Radiances
Band 1
Band 2
Band 3
Band 4
Band 5
- GAC Cutoff
GAC Cutoff
L_{WN} [mW cm^{-2} sr^{-1} um^{-1}]
2.0
1.5
1.0
0.5
0.0
0
200
400
600
800
1000
1200
Pixel